Progress In Electromagnetics Research B, Vol. 49, 55–76, 2013

DESIGN OF DUAL POLARIZED ASYMMETRICALLY FED SLOTTED RECTANGULAR PRINTED MONOPOLE ANTENNA

Raghupatruni V. S. Ram Krishna[1] and Raj Kumar[2, *]

[1]DIAT (Deemed University), Girinagar, Pune 411025, India

[2]ARDE, Pashan, Pune 411041, India

Abstract—A novel design of a CPW fed printed monopole antenna for dual polarization applications is proposed in this paper. The monopole is formed of a rectangular patch embedded with a hour-glass shaped slot. In a modified version of the antenna, an additional spiral shaped slot is incorporated in the ground plane. The overall dimensions of the antenna are kept at 40×40 mm. The impedance bandwidth achieved by the first antenna is 123% from 2.5 GHz to 10.5 GHz which is further increased to 145.5% at the center frequency of 11 GHz with the second antenna. A low polarization ratio (< 10 dB) arising from increased cross-polarization is obtained in the frequency band of 4 GHz to 10 GHz making the antenna useful for dual-polarization applications in this band.

1. INTRODUCTION

Among the several methods used for optimizing the channel capacity and enhancing reliability of data transmission, multi-input, multi-output (MIMO) has proved to be one of the best techniques. MIMO can be achieved by spatial diversity, pattern diversity or polarization diversity [1]. In spatial diversity, a number of transmitting antennas offer multiple paths (angles) for data transmission while in pattern diversity, the collocated antennas have different radiation patterns. Polarization diversity is achieved with a single antenna capable of generating multiple polarizations and is preferred over other forms as it can be realized with a lower installation cost. In one of the common forms of polarization diversity vertical and horizontal polarized waves obtained using a dual-polarized antenna are propagated in different

Received 17 January 2013, Accepted 12 February 2013, Scheduled 15 February 2013

* Corresponding author: Raj Kumar (raj34_shivani@yahoo.co.in).

directions ensuring transmission of signals uncorrelated to each other. Dual-polarized antennas can also be designed for circular polarizations (Left Handed/Right Handed) and slant polarizations ($+45°/-45°$) and can also be used to combat multi-path effects in a fading environment.

Dual polarized antennas can be realized with one-port or two-port configurations. In case of the latter, each port is designed to provide one of the two orthogonal polarizations (vertical/horizontal, LHCP/RHCP, $+45°/-45°$) while the former can be designed to provide different polarizations in different directions, different planes or at different frequencies and can have simple structures or use elements offering reconfigurability like PIN diodes and micro electromechanical system (MEMS) switches. However the use of MEMS switches makes the structure complicated and not easily embeddable with portable electronic devices.

A number of dual-polarized antenna designs based on the microstrip geometry with two port [2–7] and one port [8–11] have been reported in the available literature. A dual port patch antenna with meandering probes designed for GSM1800 and CDMA1900 applications was presented in [2]. The two ports are capable of generating the two orthogonal slant polarizations ($\pm 45°$). Another antenna for orthogonal slant polarization was proposed in [3], where pairs of petaloid patches printed on FR4 substrate were fed by coaxial probes through air-bridges and the intended usage band was from 1.71 GHz to 2.17 GHz. A cross-shaped patch antenna with four parasitic squares surrounding it and excited by diagonally placed ports was presented in [4], while the combination of an electrically fed patch and a magnetically coupled loop for $0°$ and $90°$ polarizations was discussed in [5]. A CPW fed monopole with an additional orthogonally placed microstrip feed on the other side for realizing horizontal polarization was proposed in [6]. A 4 port antenna capable of achieving X, Y, θ and ϕ polarizations was reported in [7]. Among some of the single-feed antennas, [8] presented a T-shaped feedline exciting a printed dipole and offering circular and linear polarizations in two separate bands. A CPW fed slot antenna with a halberd shaped tuning stub at the end of the feed line was proposed in [9]. Two corner slots were designed for obtaining LHCP/RHCP in two narrow bands centered at 2.5 GHz and 3.5 GHz. A printed monopole antenna with a L-shaped slot on the ground plane was presented in [10]. The polarization reconfigurability was achieved with the help of two PIN diodes, one along the microstrip line and one along the L-shaped slot. A square patch antenna fed from one of its corners was designed to achieve two different polarizations at the operating frequencies of 12.25 GHz and 14.5 GHz in [11]. The antennas described above suffer

from a lack of simplicity in design and designed to offer multiple (linear and circular) polarizations in two different narrow frequency bands.

In the present work, a printed monopole antenna design is explored for dual polarization characteristics. The monopole is a preferred structure for ultra-wideband applications as it offers wider bandwidth, nearly Omni-directional radiation patterns required in most portable devices like mobile phones and a seamless integration with the adjacent RF circuitry. Among the various shapes available for design, a rectangular patch is selected and chamfered at one of its corners. Further, an hour glass shaped slot is etched at the center of it. A CPW-feed is used for exciting the monopole. A modified version of the antenna for enhanced impedance bandwidth is also presented. The design and simulation of both the antennas are carried out using two different electromagnetic software namely the Ansoft High Frequency Structure Simulator (HFSS) and the CST Microwave Studio. The antenna structure, a description of the simulated and measured results and a brief theoretical analysis of the underlying electromagnetic phenomena is presented in the subsequent sections.

2. ANTENNA STRUCTURE

The geometry of the proposed antenna in its basic (Antenna-I) and modified (Antenna-II) version is shown in Fig. 1. A substrate of thickness $h = 1.58\,\text{mm}$ and made of FR4 Epoxy material having a relative permittivity $\varepsilon_r = 4.3$ and loss tangent $\tan\delta = 0.0019$ is utilized. The dimensions of the substrate are fixed at $40\,\text{mm} \times 40\,\text{mm}$ to keep the antenna compact. The monopole is in the shape of a

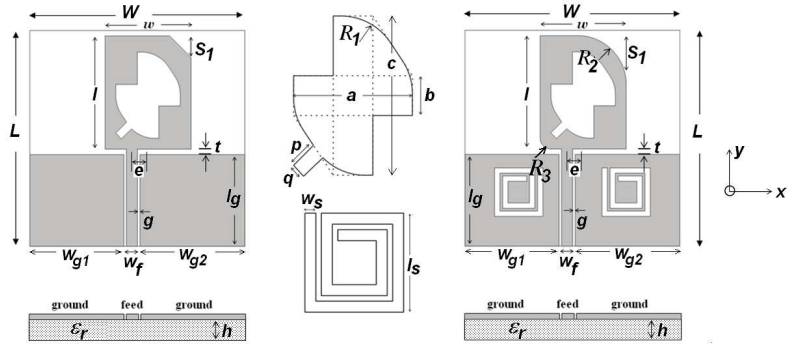

Figure 1. (a) Structural details of the proposed antenna and (b) its modified version.

rectangular patch of size $l \times w$ mm and shifted to the right hand side of the substrate center by 2 mm. The patch length 'l' is chosen to give a lower cut-off frequency near 2.5 GHz while the patch width 'w' is optimized to get the best return loss characteristic. The upper right corner of the rectangle is chamfered at a width equal to s_1. To obtain the dual-polarization characteristics, an hour glass shaped slot is etched on this rectangular patch. As shown in the figure, the slot is formed by constructing two rectangles perpendicular to each

Table 1. Optimized dimensions (in mm) of the proposed antenna.

S. No	Parameter	Antenna-I (Dimensions in mm)	Antenna-II (Dimensions in mm)
1	W	40	40
2	L	40	40
3	w	16	16.5
4	l	21	19
5	s_1	4	-
6	a	12	12
7	b	4	4
8	c	16	16
9	R_1	6	6
10	R_2	-	9
11	R_3	-	2
12	p	2.82	2.82
13	q	1.56	1.56
14	w_s	-	1
15	l_s	-	6
16	e	3	3
17	t	1	1
18	l_g	17	17
19	w_{g1}	17.5	17.5
20	w_{g2}	19.5	19.5
21	w_f	2	2
22	g	0.5	0.5
23	h	1.58	1.58

other. The horizontally placed rectangle has dimensions $b \times a$ while the vertically placed rectangle has dimensions equal to $c \times b$ mm. The cross shaped slot so formed is further modified by etching out the triangular areas at the bottom left corner and the top right corner. Finally, all the inner corners are blended with circular arcs of radii R_1. A small rectangular stub of dimensions $p \times q$ mm is added to the hour glass shaped slot. The feed line is a CPW of width 'w_f' mm and printed on the same side of the substrate as the slot loaded monopole. Its placement is made asymmetric with respect to the two ground planes. The displacement of the feed line from the center of the rectangular monopole is denoted by 'e' and its optimized value is equal to 3 mm. Another parameter in the design which has to be optimized to ensure good return loss performance is the vertical separation between the patch and the ground plane. This parameter is denoted by 't' and its optimal value is found to be equal to 1 mm.

In the improved version of the antenna, two spiral shaped slots are etched on the left and right halves of the ground plane. The spirals have opposite sense of rotation. Each spiral consists of two turns of width 'w_s' and inscribed in a square of length 'l_s'. In addition to the above modification to the ground plane, in this version of the antenna, the upper right and lower left corners of the rectangular patch are blended instead of chamfered. The radii of the circular arcs used for the purpose are R_2 and R_3 respectively. The dimensions of all the parameters of both the antennas are listed in Table 1.

3. SIMULATED AND MEASURED RESULTS

The design and simulation of the two antennas were carried out using two different electromagnetic software, namely; the Ansoft High Frequency Structure Simulator (HFSS) and the CST Microwave Studio. HFSS is based on the finite element method while the

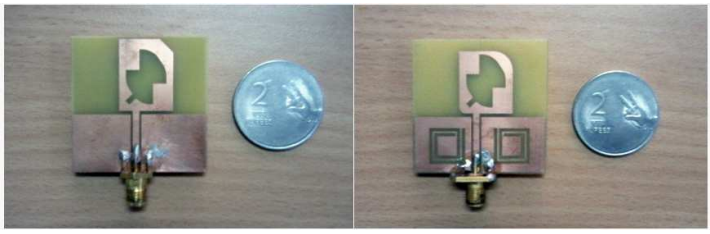

Figure 2. Photograph of the fabricated prototypes of the proposed antenna.

CST Microwave Studio employs the finite integration technique. Experimental validation of the two designs was done by fabricating the two prototypes (shown in Fig. 2) and measuring the frequency response on a Rohde & Schwarz Vector Network Analyzer (ZVA-40). A plot of the reflection coefficient (S_{11}) magnitude as simulated using the two software and compared with the measured response for Antenna-I and Antenna-II are shown in Fig. 3 and Fig. 4, respectively.

It can be seen from the figures that the two simulated responses are in good agreement with each other. Also, a similarity in the behavior of the measured response can be seen although there is some difference in the magnitude of the peaks. The slight difference between the two simulated results is because of the difference in the numerical technique used by the respective software. The difference between the measured results and the simulated results is due to the fabrication tolerances, connection mis-alignment and uncertainty in the substrate thickness and the impedance response of the Sub-Miniature Version 'A' (SMA) connectors used.

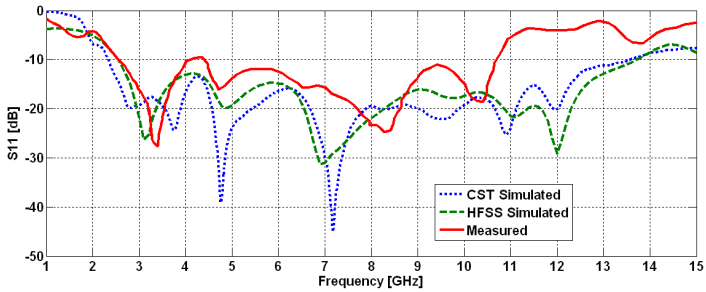

Figure 3. Simulated and measured return loss of Antenna-I.

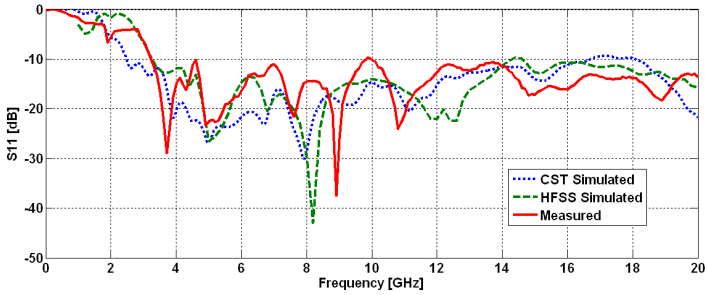

Figure 4. Simulated and measured return loss of Antenna-II.

For antenna-1, the dips in the response (resonances) are seen to occur at 2.8 GHz, 3.75 GHz, 4.75 GHz, 7.2 GHz, 9.5 GHz and 10.9 GHz (CST simulation). An overlap of these resonances provides the ultra-wideband nature of the overall response. The effect of adding spiral shaped slot in the ground plane is seen to shift some of the above resonant frequencies to the lower side while at the same time adding a few higher resonances.

3.1. Dual Polarization

To study and compare the polarization properties of the two antennas, the polarization ratio (difference between the vertical and horizontal component) along the boresight direction for the two antennas as simulated by CST is plotted as shown in Fig. 5. The polarization ratio of each of the antennas was measured in the in-house anechoic chamber and the results are shown in Fig. 6 and Fig. 7.

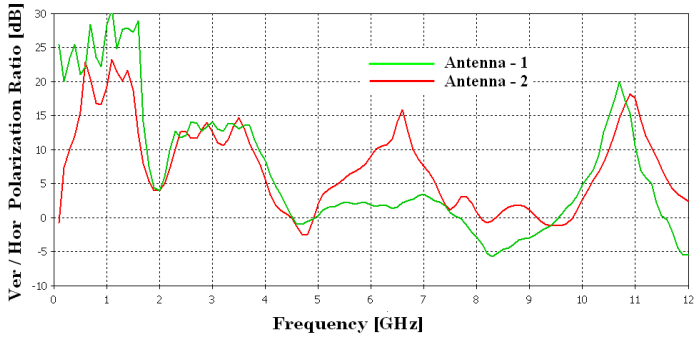

Figure 5. Comparison of the simulated polarization ratio for Antenna-1 and 2.

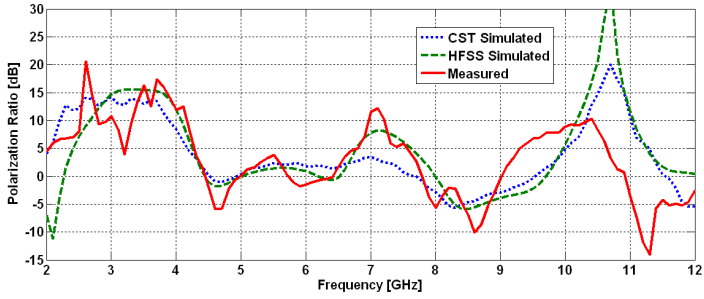

Figure 6. Measured polarization ratio of the Antenna-1.

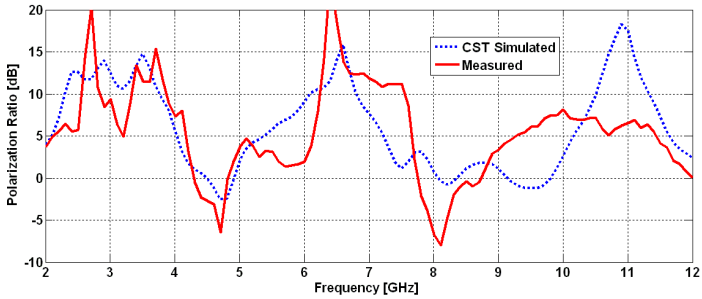

Figure 7. Measured polarization ratio of the Antenna-2.

Table 2. Resonance frequencies (GHz) of S_{11}-curve for different stages of Antenna-I.

Resonance	Stage-I (Sym. Feed)	Stage-II (Feed Shifted)	Stage-III (Slot Loaded)
f_1	2.87	2.9	2.87
f_2	3.9	4.0	3.72
f_3	Not Excited	Not Excited	4.75
f_4	7.2	7.6	7.2
f_5	Not Excited	9.75	9.5
f_6	Not Excited	Not Excited	10.9
f_7	Not Excited	12.2	12.0

It is seen that from 2 GHz to about 4 GHz, the difference in the two orthogonal components is between 10 to 15 dB with the vertical polarization dominating. The polarization ratio drops below 5 dB near 4 GHz and stays within 5 dB up to about 10 GHz for Antenna-1. This region (from 4 GHz to 10 GHz) can be defined as the useful band. The polarization ratio characteristic of Antenna-2 is nearly same as Antenna-1 except for an increase in the ratio between 5.5 GHz to 7.0 GHz and this may be considered as the effect of the spiral slot etched on the ground plane.

4. THEORETICAL ANALYSIS

4.1. Reflection Coefficient

The return loss characteristics of the Antenna-1 can be explained by observing the evolution process of the antenna basically starting with

a symmetrically fed simple rectangular patch and then modifying it by shifting the feed line and finally the addition of an hour glass shaped slot.

The resonant frequencies as observable from Fig. 8 for the three stages are listed in Table 2. A plot of the surface current at the resonant frequencies for the symmetrically fed, feed shifted and the final stage of Antenna-1 (Stage-1, Stage-2 and Stage-3) is shown in Fig. 9, Fig. 10 and Fig. 11 respectively. The lowest frequency excited in all the cases is near 2.9 GHz which approximately corresponds to that obtained from the equation for a printed monopole (1).

$$f_l = \frac{0.25 \times 300}{l + t + (w/2\pi)} \tag{1}$$

The contributing factor for the second resonance near 4 GHz is the active width of the ground plane which is dependent on the coupling between the lower edge of the patch and the upper edge of the ground plane. The third resonance which is prominent by its absence in the first two stages (not having the slot) is generated by the slot and

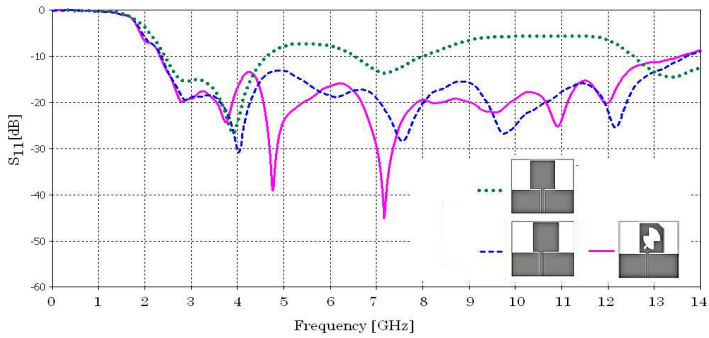

Figure 8. Evolution of Antenna-I (simulated return loss).

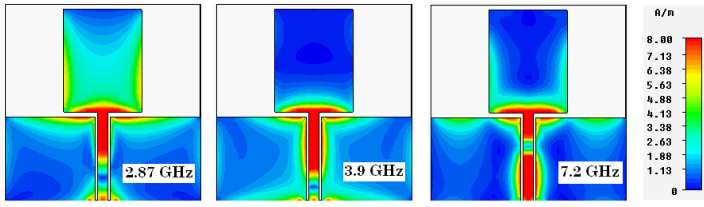

Figure 9. Surface current (magnitude) plot for symmetrically fed antenna.

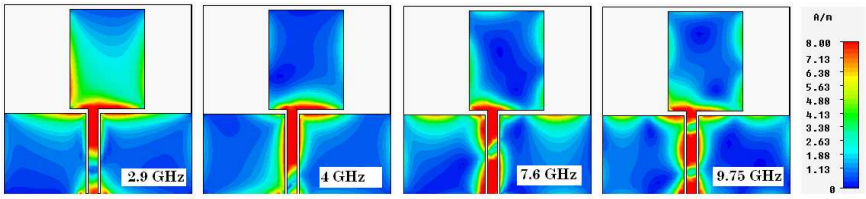

Figure 10. Surface current (magnitude) plot for feed shifted antenna.

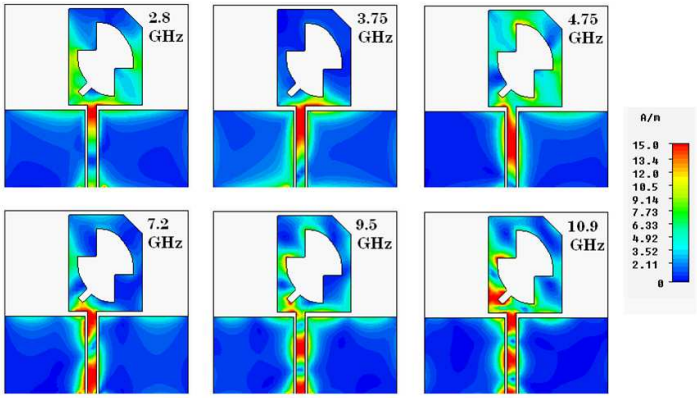

Figure 11. Surface current distribution at different resonances for Antenna-I.

magnitude governed by the effective slot perimeter. Surface current plot at different resonances of Antenna-II is given in Fig. 12.

4.2. Polarization Ratio

It is a known fact that a simple printed monopole structure displays a dominance of vertical polarization component. The basic objective in the present antenna design was to achieve dual polarization by increasing the cross (horizontal) polarization. A study similar to that for the reflection coefficient was undertaken to see the effect of various modifications (stages of evolution) on Antenna-I and the results are shown in Fig. 13 where the polarization ratio along the bore sight direction is plotted as a function of frequency.

It is quite obvious from this figure that a simple unperturbed rectangular patch monopole gives a pure vertically polarized field and the cross polar difference is very high (about 40 dB). The effect of shifting the feed to one side creates an asymmetry (in the ground

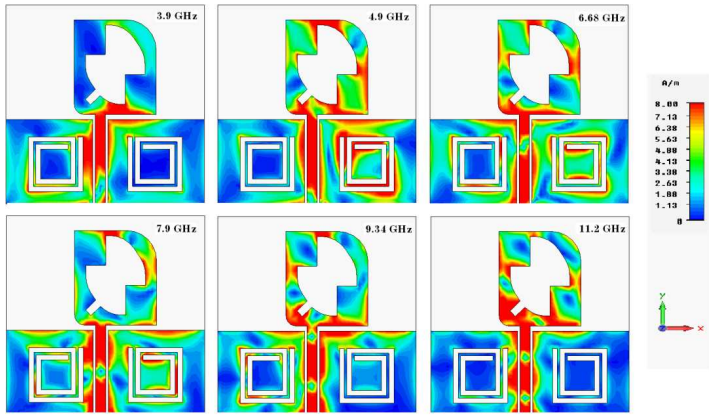

Figure 12. Surface current distribution at different resonances for Antenna-II.

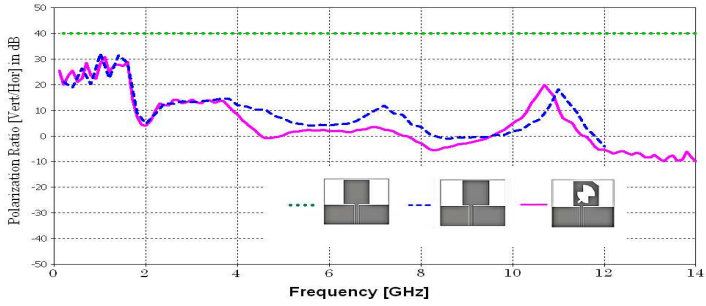

Figure 13. Evolution of Antenna-I (simulated polarization ratio).

planes as well) whose effect can be immediately seen to increase the cross polarization such that the ratio drops to below 20 dB after about 1.7 GHz). Introduction of the slot in the rectangular patch further increases the cross polar component and a band of 4 GHz to 10 GHz is obtained where the ratio stays below 10 dB. The effect of shifting the feed in creating an increased horizontal component can be seen from Fig. 14 where current plots for the simple and feed shifted stages are shown.

A few observations from the vector current plot for Antenna-1 shown in Fig. 15 help in better understanding. At 2.8 GHz, the currents on the patch and on the ground are mostly in the vertical direction with the latter dominating the former, and hence the resultant polarization is largely vertical. The patch current increases

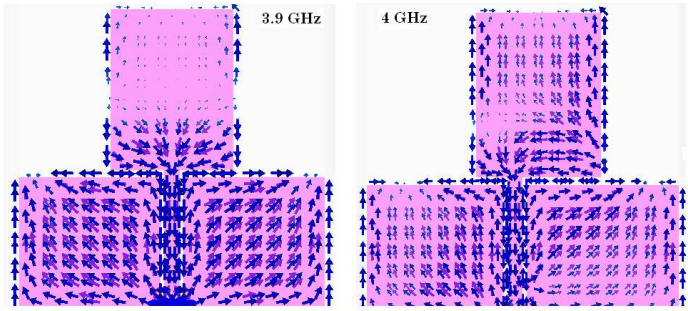

Figure 14. Current distribution for the simple and feed shifted stages.

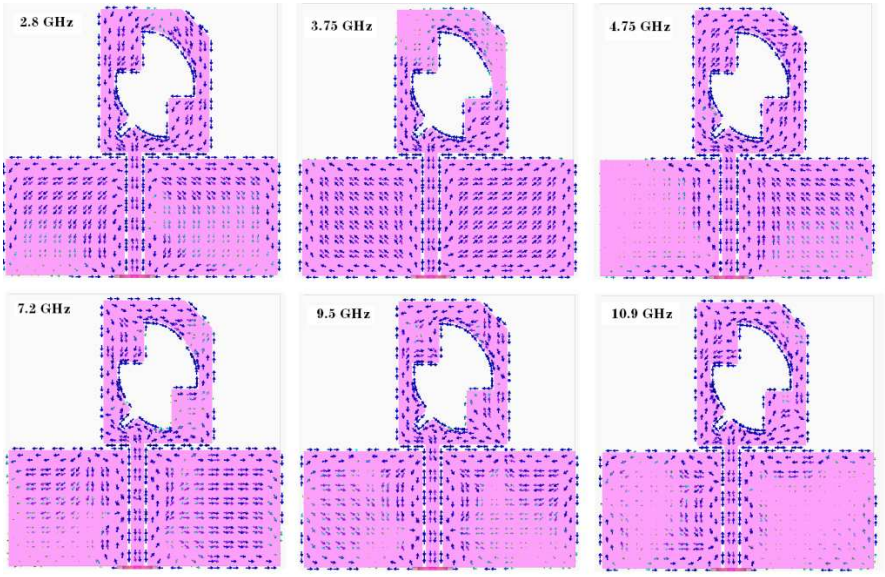

Figure 15. Vector current plot at resonant frequencies for Antenna-I.

at 3.75 GHz and the ground current shows rotation. The currents on the left and right ground plane have an opposite sense of rotation and the horizontal components seem to cancel each other. However the currents on the two sides are slightly unequal in magnitude and hence the cross polarization increases. A maximum enhancement in the cross-polarization is seen at 4.75 GHz where the currents on the right plane largely dominate the currents on the left plane. Further at this frequency the patch current also shows rotation adding to the

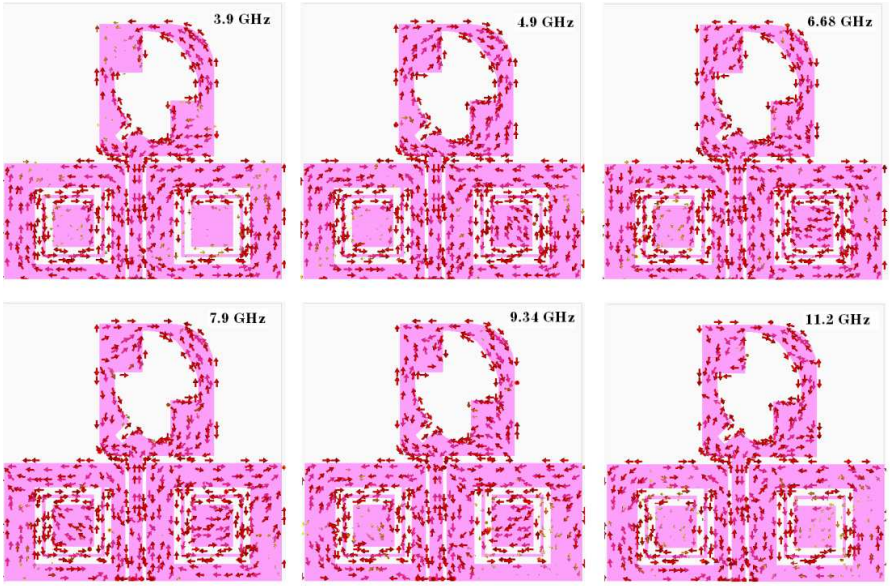

Figure 16. Vector current plot at resonant frequencies for Antenna-II.

horizontal polarization. As frequency is further increased, the current distribution on the ground planes again become equal resulting in a larger cross polar difference. Hence it can be concluded that at the frequency at which the slot resonates, a maximum amount of asymmetry is created in the induced ground plane currents resulting in a small polarization ratio. The vector current plot for Antenna-2 is shown in Fig. 16.

5. PARAMETRIC STUDY

As a continuation of the previous section, the results of the parametric study on some of the parameters of Antenna-1 are presented in this section.

5.1. Effect of Varying the Patch Dimensions

The effects of increasing the patch length 'l' and the patch width 'w' on the return loss and polarization ratio (difference between the vertical and horizontal components) are shown in Fig. 17 and Fig. 18 respectively. The first resonance near 2.9 GHz is only affected by the length and it shifts to the lower side with an increase in the length as

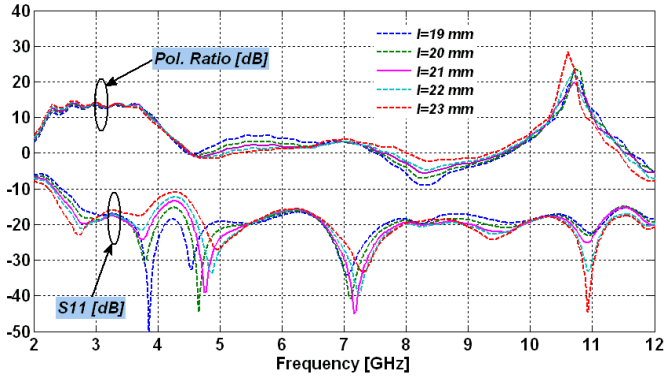

Figure 17. Effect of patch length 'l' on S_{11} and polarization ratio (Antenna-I).

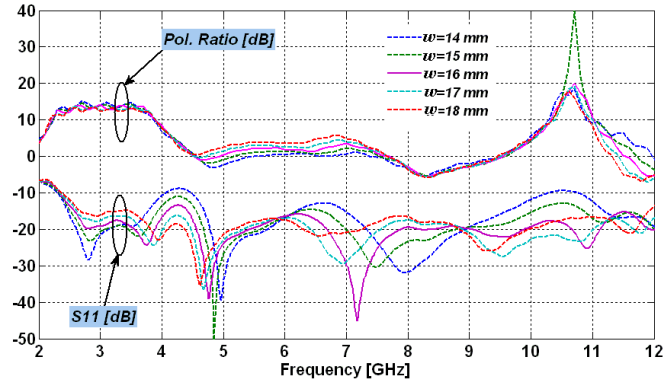

Figure 18. Effect of the patch width 'w' on S_{11} and polarization ratio (Antenna-I).

expected. The increase in patch length and width affect the second and third resonances in mutually opposing manner. While the second resonant frequency decreases with an increase in the patch length, it increases with an increase in the patch width. On the contrary, the third resonant frequency increases with an increase in the patch length while decreasing with an increase in the patch width. Thus it can be concluded that decreasing the patch length has a similar effect as increasing the patch width. A larger aspect (w/l) ratio relaxes the enforcement of patch current along the slot periphery and distributing it in the region between the patch and the slot. This causes an increase

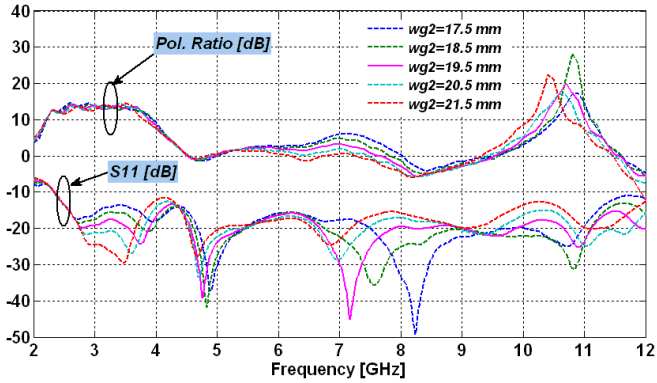

Figure 19. Effect of the ground plane width 'w_{g2}' on S_{11} and polarization ratio (Antenna-I).

in the current path and the third resonance is seen to shift towards the lower side.

5.2. Effect of Varying Ground Width w_{g2}

The effect of the ground width is shown in Fig. 19. It is seen that an increase in the width of the ground plane shifts the second and third resonances to the lower side. The second resonance is directly related to the width of the ground plane while the explanation for the effect on the third resonance is similar to that discussed for an increase in the patch width. Increasing the ground width also leads to a higher horizontal component and reduced cross-polar ratio as seen in the figure near 7 GHz.

5.3. Effect of Shifting the Feed

The feed position plays a very important role in the overall design of the proposed antenna and its effect on the return loss and the polarization ratio can be clearly seen from Fig. 20. An increase in the feed shift introduces a higher degree of asymmetry and consequently increases the cross polarization and thus reducing the cross-polar ratio as noticed from the figure. It causes no significant displacement of the first and second resonance as the mode lengths practically remain the same. A more dramatic effect of the feed shift can however be seen on the overall magnitude of the reflection coefficient. It is observed that more negative values of return loss are attained with larger shifts in the feed position indicating a better impedance matching with the feed line. A

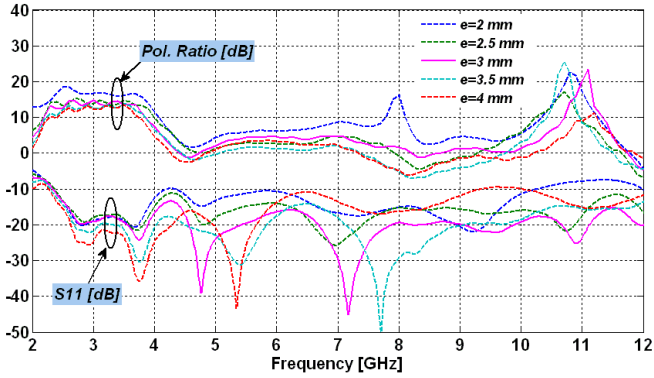

Figure 20. Effect of the feed shift 'e' on S_{11} and polarization ratio (Antenna-I).

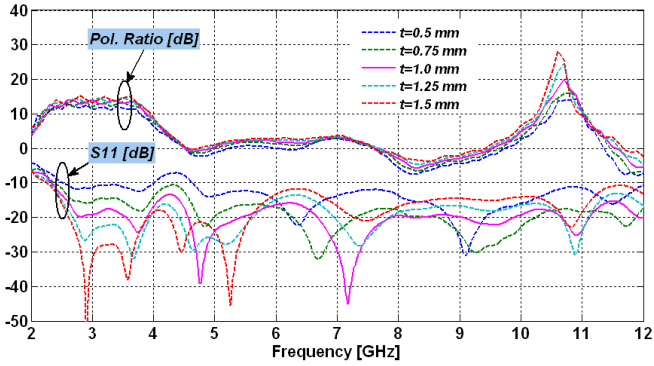

Figure 21. Effect of the patch-ground separation 't' on S_{11} and polarization ratio (Antenna-I).

similar effect of shifting the feed can be seen on the performance of Antenna-II.

5.4. Effect of Varying the Separation between Patch and Ground

While the feed shift is the most important parameter determining the cross polarization level, the separation between patch and ground plays a crucial role in obtaining wider impedance bandwidth. As seen from Fig. 21, even a small change in the separation 't' can push the return loss curve above the -10 dB threshold. A reduction in the separation

between the patch and the ground plane leads to a tighter coupling between the two and leads to more of the patch and ground currents to concentrate on the horizontal edges. This affects the edge impedance of the patch resulting in a larger mismatch (poor return loss) and increases the second resonance by reducing the vertical component of the current path. On the other hand, with a larger separation, the strength of the harmonic resonances decreases due to reduced dimensions and again a satisfactory behavior of the return loss may not be obtained. This makes the separation a parameter to be optimized.

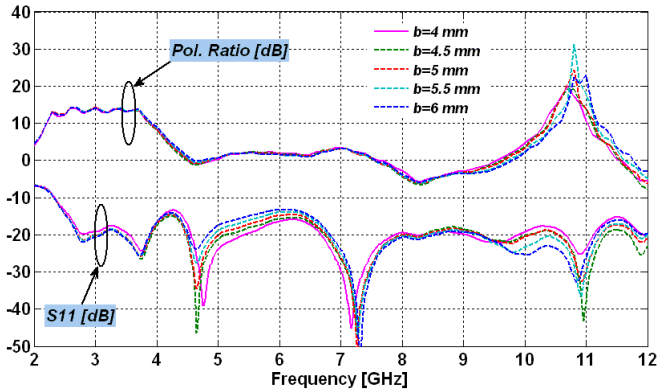

Figure 22. Effect of the slot width 'b' on S_{11} and polarization ratio (Antenna-I).

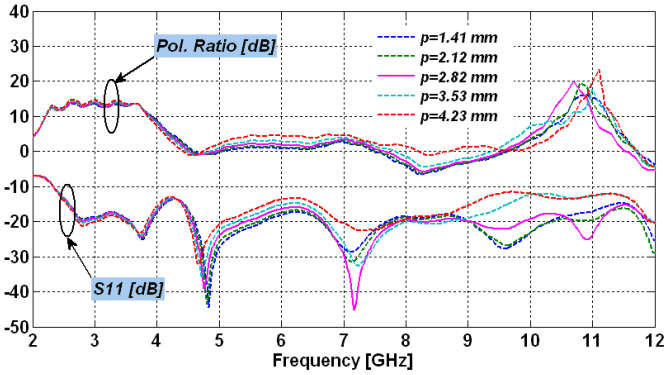

Figure 23. Effect of the slot stub length 'p' on S_{11} and polarization ratio (Antenna-I).

5.5. Effect of Varying the Slot Size and the Slot Stub Length

The effect of increasing the slot dimension 'b' has a minimal effect on the cross polarization (Fig. 22). The resonance at 4.75 GHz shifts slightly to the lower side consequent to the increase in the slot perimeter. Other fundamental resonances remain unaffected. Similarly, an increase in the slot stub length 'p' increases the slot perimeter and hence causes a reduction in the slot induced third resonant frequency (Fig. 23).

6. RADIATION PATTERNS, GAIN AND EFFICIENCY

6.1. Radiation Patterns

The co-polarized radiation patterns in the E-plane and H-plane for Antenna-1 and Antenna-2 are shown in Fig. 24 and Fig. 25 respectively. The patterns follow a typical monopole-like behavior at lower frequencies showing omnidirectionality in the H-plane and resembling the figure of eight in the E-plane. The effect of increased cross polarization and enhanced higher order modes is seen to

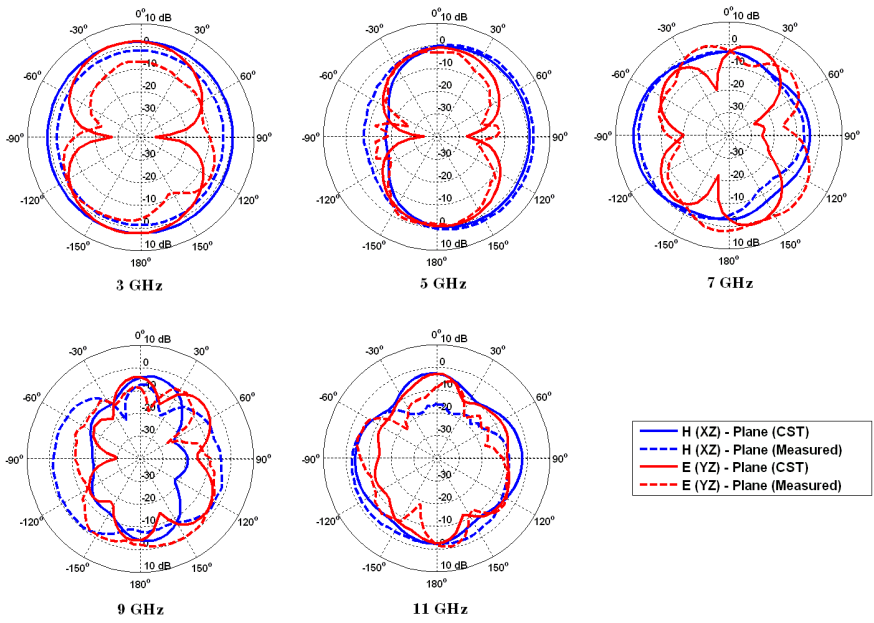

Figure 24. Simulated & measured radiation patterns of Antenna-I.

deteriorate the radiation patterns at the higher frequencies. The agreement between the measured patterns and the simulated ones is good at the lower frequencies while slightly becoming poor at higher frequencies.

6.2. Peak Gain and Radiation Efficiency

The measured peak gain of the proposed antennas is shown alongside the simulated gain in Figs. 26 and 27 while the simulated radiation

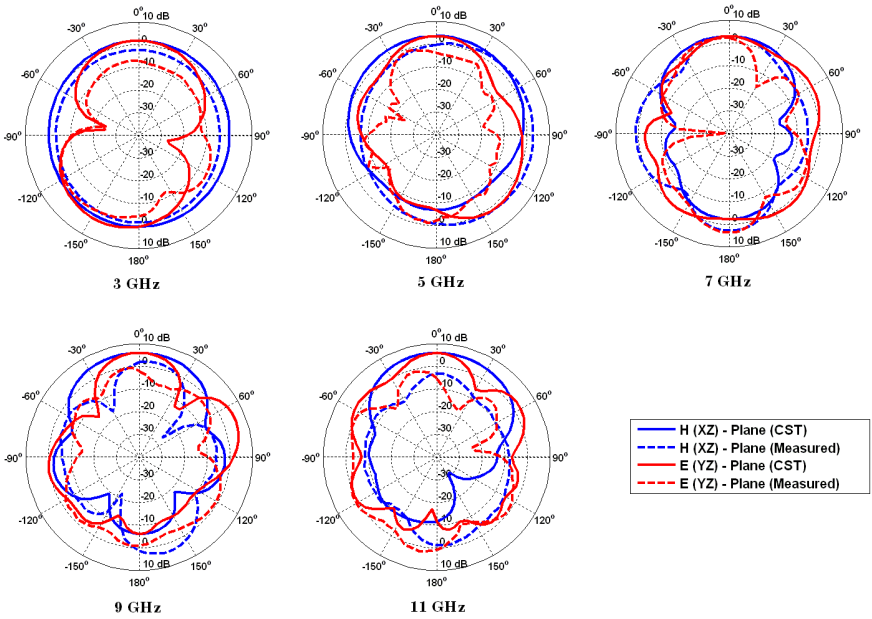

Figure 25. Simulated and measured radiation patterns of Antenna-II.

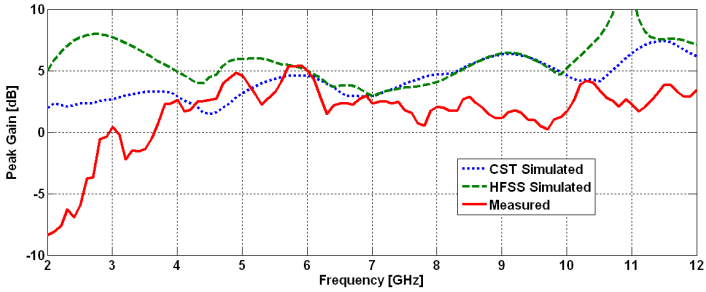

Figure 26. Simulated & measured peak gain for Antenna-I.

efficiency for Antenna-1 is shown in Fig. 29. It can be seen that the simulated peak gain of Antenna-1 remains between 2 dB and 3 dB over much of the useful bandwidth and shows a slight increase at higher frequencies which is due to an increase in the effective area for radiation contributed by smaller wavelengths. There is also a slight disagreement between the measured and simulated gains and this may be due to the additional losses in the measurement system not incorporated in simulations which mostly approximate directivity. The low value of the measured gain in the region of 2 to 4 GHz for both the antennas can be further attributed to the poor gain characteristics of the reference horn antenna employed in the measurement system (Schwarzbeck BBHA 9120C) as shown in Fig. 28. Compared to the Antenna-1, the gain (simulated and measured) of Antenna-2 is slightly higher at higher frequencies. This correlates with the fact that Antenna-2 also has a better return loss characteristic than Antenna-1 at higher frequencies (wider bandwidth).

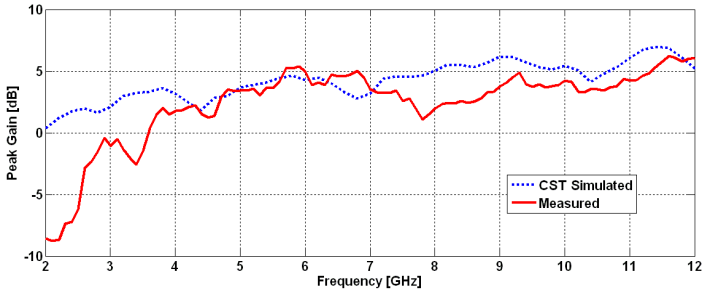

Figure 27. Simulated & measured peak gain for Antenna-II.

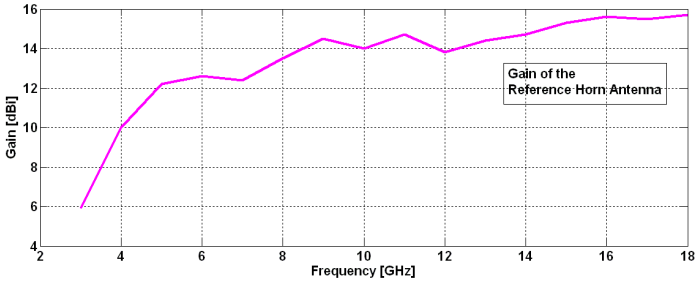

Figure 28. Gain of the reference horn antenna used in the measurement system.

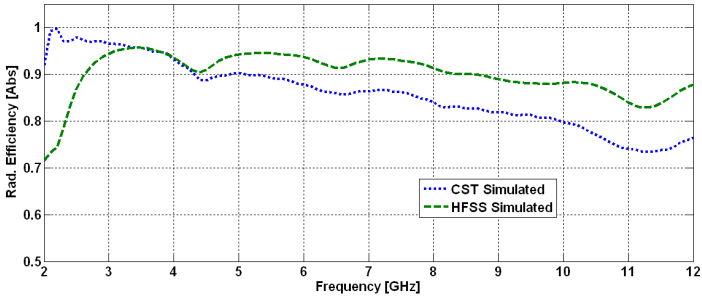

Figure 29. Simulated radiation efficiency for Antenna-1.

7. CONCLUSION

The design of a dual polarized antenna utilizing a rectangular patch shaped monopole is presented in this paper. The patch is loaded with a dumb bell shaped slot for achieving horizontal polarization. Further modification is provided by embedding a spiral shaped slot in the ground plane. The impedance bandwidth achieved is 123% (from 2.5 GHz to 10.5 GHz) without the spiral slot and about 145.5% (from 3 GHz to 19 GHz) with the spiral slot. The region of low cross polarization ratio is from 4 GHz to 10.5 GHz. The antenna will be useful for applications requiring dual polarization capability in the 4 GHz to 10 GHz band and for vertically polarized applications in the remaining band.

ACKNOWLEDGMENT

The authors would like to thank the reviewers for their comments and useful suggestions. The first author is a doctoral student at the Defense Institute of Advanced Technology, (Deemed University), Pune, India and acknowledges the financial support provided by the institute for carrying out the research work.

REFERENCES

1. Khalegi Bisaki, H., *MIMO Systems, Theory and Applications*, InTech Open Science Publications, 2011.
2. Lai, H.-W. and K.-M. Luk, "Dual polarized patch antenna fed by meandering probes," *IEEE Transactions on Antennas and Propagation*, Vol. 55, No. 9, 2625–2627, September 2007.

3. Liu, C., J.-L. Guo, Y.-H. Huang, and L.-Y. Zhou, "A novel dual-polarized antenna with high isolation and low cross polarization for wireless communication," *Progress In Electromagnetic Research Letters*, Vol. 32, 129–136, 2012.
4. Pinchera, D. and F. Schettino, "A dual-polarized parasitic patch antenna for MIMO systems," *Proceedings of the 39th European Microwave Conference*, 642–644, Rome, Italy, September 2009.
5. Xie, J.-J., Y.-Z. Yin, J. Ren, and T. Wang, "A wideband dual-polarized patch antenna with electric probe and magnetic loop feeds," *Progress In Electromagnetic Research*, Vol. 132, 499–515, 2012.
6. Wang, X., W. Chen, Z. Feng, and H, Zhang, "Compact dual-polarized antenna combining printed monopole and half slot antenna for MIMO applications," *IEEE International Symposium on Antennas and Propagation Proceedings*, 1–4, Beijing, China, June 2009.
7. Yang, S.-L. S., K.-M. Luk, H.-W. La, A.-A. Kishk, and K.-F. Lee, "A Dual-polarized antenna with pattern diversity," *IEEE Antennas and Propagation Magazine*, Vol. 50, No. 5, 71–79, December 2008.
8. Bao, X. L. and M. J. Ammann, "Wideband dual-frequency dual-polarized dipole-like antenna," *IEEE Antennas and Wireless Propagation Letters*, Vol. 10, 831–834, 2011.
9. Zhang, X.-Q., Y.-C. Jiao, and W.-H. Wang, "Compact dual-band dual-sense circularly-polarized CPW-fed slot antenna," *Progress In Electromagnetic Research Letters*, Vol. 34, 197–205, 2012.
10. Amini, M. H., H. R. Hassani, and S. Mohammad Ali Nezhad, "A single feed reconfigurable polarization printed monopole antenna," *6th European Conference on Antennas and Propagation Proceedings*, Prague, Czech Republic, March 2012.
11. Wang, M., W. Wu, and D.-G. Fang, "Uniplanar single corner-fed dual-band dual-polarization patch antenna array," *Progress In Electromagnetic Research Letters*, Vol. 30, 41–48, 2012.